

ONLINE INSTANTANEOUS FREQUENCY ESTIMATION UTILIZING EMPIRICAL MODE DECOMPOSITION AND HERMITE SPLINES

Franz R. Holzinger, Martin Benedikt

VIRTUAL VEHICLE Research Center
Area E - Electrics/Electronics and Software
Inffeldgasse 21/A, 8010 Graz, Austria

ABSTRACT

Most of the available frequency estimation methods are restricted for the application to signals without a bias or a carrier signal. For offline analysis of a signal an existing carrier may be determined and eliminated. However, in the case of online computations the carrier is not accurately known a priori in general. An error in the carrier signal directly affects the accuracy of the subsequent instantaneous frequency estimation approach. This article focusses on the online instantaneous frequency estimation of non-stationary signals based on the empirical mode decomposition scheme. Especially Hermite spline interpolation of samples for empirical mode decomposition is addressed. Hermite splines enables the definition of enhanced boundary conditions and leads to an effective online instantaneous frequency estimation approach. Throughout the article algorithmic details are examined by a theoretical example.

Index Terms— EMD, online, spline interpolation, boundary condition

1. INTRODUCTION

In common, the frequency content of a non-stationary signal at hand is determined by classical signal processing approaches. The well known representatives are the short time Fourier transformation (STFT) or the Wavelet transformation (WT). As disadvantageous fact, both approaches lead to a bad resolution in the time domain or in the frequency domain: the time-frequency uncertainty principle by Heisenberg, makes it difficult to assign a frequency value to a given point in time. In 1998, Huang proposed a data-driven method, the empirical mode decomposition (EMD), which decomposes a signal into several components with special properties [1, 2]. Subsequent application of the Hilbert transformation to the resulting mode leads to an analytical signal representation and a very accurate instantaneous frequency computation - also in time. This approach is referred to as Hilbert-Huang transformation (HHT) and outperforms classical signal processing schemes regarding the achievable resolution in time and frequency domain [1, 3].

Because of the limited observation length of the signal and numerical effects instead of the Hilbert transformation other approaches are utilized to determine the instantaneous frequency. For example, in [4] an auto-regressive (AR) estimation approach is used and some algorithmic details concerning the EMD are discussed. This paper is devoted to address algorithmic issues regarding an online version of the EMD. The proposed improvements solve some critical problems and lead to a promising approach for online instantaneous frequency estimation.

Section 2 presents a representative online frequency estimation method. The EMD scheme and its problems are discussed in Section 3. Section 4 is devoted to well-known online computation problems and the application of Hermite spline interpolation is proposed. In Section 5, the performance improvement regarding online EMD as well as online frequency estimation is demonstrated.

2. INSTANTANEOUS FREQUENCY ESTIMATION

As an example for the online estimation of the instantaneous frequency (IF) the *Discrete time Energy Separation Algorithm* (DESA) is used. This scheme is based on the Teager Kaiser energy operator, which is originated on the observations of Teager in 1980 and was revised by Kaiser in 1990 [5]:

$$\Psi \{y(t)\} = \dot{y}(t)^2 - y(t)\ddot{y}(t) \quad (1)$$

The time continuously frequency estimation based on the energy operator is outlined in (2). By this equation the affect of a constant offset in the analysed signal can be illustrated. There is no impact of the bias term in the numerator because of the derivation. Otherwise, the offset is not eliminated in the denominator, which causes a frequency estimation error.

$$\omega(t) = \sqrt{\frac{\Psi \{\dot{y}(t)\}}{\Psi \{y(t)\}}} \quad (2)$$

For a discrete scheme the estimation of the frequency is defined as follows [5, 6]:

$$\omega_k \approx \arccos \left(1 - \frac{\Psi \{y_k - y_{k-1}\}}{2\Psi \{y_k\}} \right) \quad (3)$$

3. EMPIRICAL MODE DECOMPOSITION

The empirical mode decomposition (EMD) was developed by Huang to analyse non-stationary signals in the time-domain. It is solely defined by a non-linear iterative algorithm instead of mathematical formulas and separates a non-stationary signal into several components [1, 2]. The sum of the resulting components represents the original signal. The extracted components are so-called intrinsic mode functions (modes), which represent zero-mean AM-FM components, and a residuum, i.e. a trend or carrier. Each intrinsic mode function has two fundamental properties:

- The difference of the number of zero crossings and the number of extrema must be less than or equal to one
- The mean of the envelope along the maxima and the envelope along the minima must be zero at each time step

The most important fact is, that each of the individual modes is available without any carrier and carrier sensible instantaneous frequency estimation techniques may be applied directly to the extracted modes.

3.1. The EMD algorithm

The algorithm consists of two loops of iterations, where the nested iteration is referred to as sifting process [1, 2]. If a signal $h^{(p,q)}(t)$ with the indices q and p is considered, the index $q = 1, \dots, Q$ denotes the sifting process iteration and $p = 1, \dots, P$ indicates the iteration in a specific sifting operation. At the beginning of each sifting process q the signal $h^{(1,q)}(t)$ is set to an intermediate available signal $r^{(q)}(t)$. In the initial step, the original signal $y(t)$ is represented by $r^{(1)}(t)$. During processing the following steps are performed:

1. Detection of the minima $h_{m,i}^{(p,q)}(t)$ and maxima values $h_{M,i}^{(p,q)}(t)$ of the signal $h^{(p,q)}(t)$
2. Determine the envelope of the maxima $h_M^{(p,q)}(t)$ and the envelope of the minima $h_m^{(p,q)}(t)$
3. Calculate the mean $m^{(p,q)}(t)$ of the envelopes:

$$m^{(p,q)}(t) = \frac{h_M^{(p,q)}(t) + h_m^{(p,q)}(t)}{2} \quad (4)$$

4. Determine the difference between signal and mean:

$$h^{(p+1,q)}(t) = h^{(p,q)}(t) - m^{(p,q)}(t) \quad (5)$$

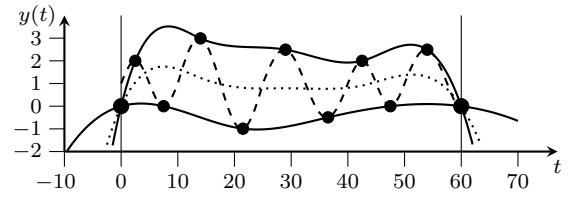
The steps 1 to 4 are repeated until the signal $h^{(p,q)}(t)$ confirms the IMF's criterions mentioned above. In this case this sifting process is finished and the result $h^{(p,q)}(t)$ represents an intrinsic mode:

$$c_q(t) = h^{(P,q)}(t) = r^{<q>} - \sum_{p=1}^P m^{<p,q>}(t) \quad (6)$$

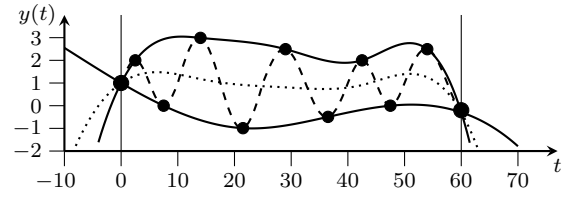
The signal for the next sifting process is calculated as follows:

$$r^{<q+1>}(t) = r^{<q>}(t) - h^{(P,q)}(t) \quad (7)$$

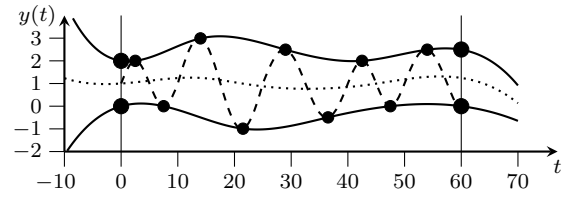
The EMD process stops if no additional mode can be extracted. In this case, the signal $r^{<q>}(t)$ has monotonic behavior and represents the trend. The sum of all extracted modes and the resulting trend represents the original signal $y(t)$ and thus, the EMD is independent of the behavior of the decomposition algorithm. The extracted modes themselves depend on the detection of the extrema, the kind of interpolation used to calculate the envelopes and boundary conditions [1, 2, 4]. The common boundaries are discussed subsequently.



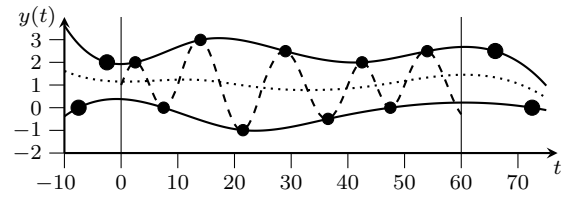
(a) Boundary to zero



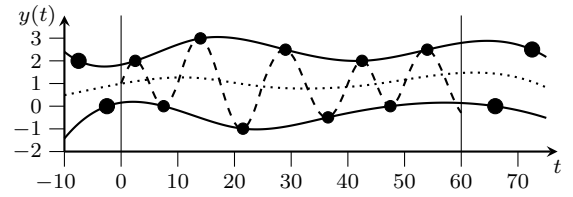
(b) Boundary to interval limit value



(c) Boundary to extrema



(d) Mirroring of the extrema



(e) Skew symmetric mirroring

Fig. 1. Envelopes by using different boundary conditions

3.2. Boundary conditions

The envelopes are defined by the minima and maxima values and represent an interpolation between the detected extrema. As disadvantageous fact, the behavior of the interpolated envelopes is directly affected by the boundary condition. Especially this phenomenon has (huge) influence for short signal observation windows where only a small number of extrema is available. For example, Fig. 1 depicts the influence on the envelopes for different boundary conditions. Different boundary conditions are illustrated in Fig. 1a, 1b and 1c. As expected, there is a significant affect regarding the upper and the lower envelope. If there are extrema near the observation window edges or large offsets exist and the boundary is set to zero problems occur. Application of symmetric mirroring and skew symmetric mirroring (Fig. 1d and 1e) of the extrema at the edges of the observation window are proposed in [2,4]. By the skew mirrored approach minima and maxima alternately occurs and leads to an improved behaviour near the interval limits.

4. BLOCKWISE EMD

The previously conducted considerations are mainly connected to an offline analysis of a given signal. In this case, typically a huge number of samples is available, the boundary conditions affect only the edges at the observation window and the number of iterations performed is not critical according to the required processing time. However, for an online or realtime application during a measurement or simulation process the common EMD needs to be extended because of several algorithmic drawbacks. Basically, for online application, only a small window is analysed. The dependency of the EMD on extrema suggests, that a blockwise or windowed EMD is calculated with each new occurring maxima or minima. Furthermore, the observation window is moved with each extrema. For an online application - meaning a blockwise signal analysis - of the EMD additional problems occur [2,4]:

- New extrema influence past intervals of extracted modes
- Discontinuities at the edges of the blockwise extracted modes occur

The discontinuities result due to the use of common boundaries, because the properties of two blockwise calculated modes do not match at the edges in general. To solve the listed problems the used interpolation scheme is addressed. Hermite splines allow the definition of enhanced boundary conditions, which enables an important improvement of the online EMD algorithm. In addition to prevent the discontinuities new boundaries based on Hermite spline interpolation are proposed.

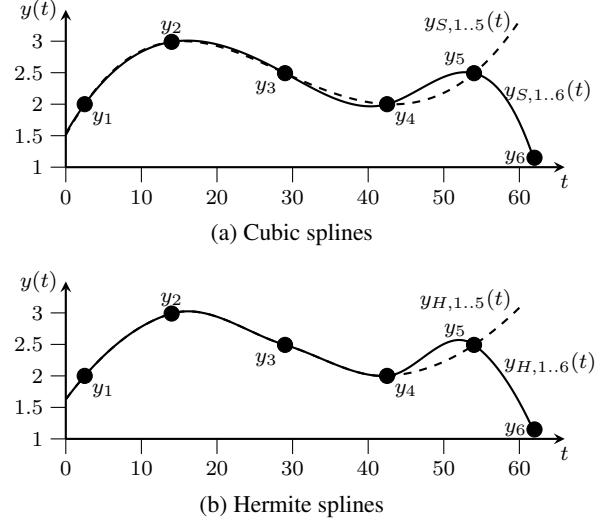


Fig. 2. Difference between cubic splines and Hermite splines

4.1. Hermite spline interpolation

Cubic splines interpolate a third order polynomial between adjacent samples. In addition to the values of the two splines at each sample point also the first and second derivation have to match. Thus, a new sample changes the interpolation over wide past intervals. This fact restricts the use of ordinary splines regarding online EMD. To avoid this effect Hermite splines are proposed for interpolation purposes [7]. Thereby, only the local derivation is of interest. The first derivation is fixed by the adjacent samples and enables a local consideration of the splines. This is a necessary (local) condition for an efficient online application of the EMD. Basically, Hermite splines are defined by

$$y_H(t) = \frac{2T_k\tau^2 - 2\tau^3}{T_k^3}y_{k+1} + \frac{T_k^3 - 3T_k\tau^2 + 2\tau^3}{T_k^3}y_k + \dots + \frac{\tau^2(\tau - T_k)}{T_k^2}d_{k+1} + \frac{\tau(\tau - T_k)^2}{T_k^2}d_k$$

where d_k represents the slope of the spline, $T_k = t_{k+1} - t_k$ and $\tau = t - t_k$, see [8]. Fig. 2 illustrates the difference between cubic and Hermite spline interpolation. Interpolated curves are depicted based on five and six samples and allows a comparison of both approaches. Especially, in the case of using Hermite splines, the interpolated signal is only affected in the interval between the last two samples y_4 and y_5 .

4.2. Boundary conditions for blockwise EMD

Concerning online (blockwise) EMD signal processing it is necessary to know the behavior on the left boundary to ensure that the mode signal has a steadily behavior. Therefore, the values and the derivations of the modes c_q must agree at the junction t_j , i.e. the left edge of the analysed block (see

Fig.3). The relation between the mode c_q and the envelopes $h_m^{<p,q>}$ and $h_M^{<p,q>}$ in (4) and (6) shows that if the mode is continuous, the envelopes must also occupy continuity at the observation limit t_j . Further, the number of sifting iterations is different for the extraction of the mode in subsequent block windows. Thus it is not expedient to define the boundaries of the envelopes for each specific iteration step. In accordance to (6) the intrinsic mode function is represented by:

$$c_q(t) = r^{<q>} - \left(\frac{1}{2} \underbrace{\sum_{p=1}^P h_M^{<p,q>}}_{H_M(t)} + \frac{1}{2} \underbrace{\sum_{p=1}^P h_m^{<p,q>}}_{H_m(t)} \right) \quad (8)$$

Instead of the properties of each envelope $h_m^{<p,q>}$ and $h_M^{<p,q>}$ during a sifting process, the sum of the upper envelopes $H_M(t)$ and the sum of the lower envelopes $H_m(t)$ are considered. The behavior of $H_m(t)$ and $H_M(t)$ of the prior observation window are used to describe the properties of the new mode at the observation limit t_j . In the first sifting iteration the values of the upper and lower envelope at the boundary are defined via

$$y_{M,0} = H_M(t_j) \quad \text{and} \quad y_{m,0} = H_m(t_j) \quad (9)$$

and the slopes at the left boundary are defined by:

$$\dot{y}_{M,0} = \left. \frac{d}{dt} H_M(t) \right|_{t=t_j} \quad \dot{y}_{m,0} = \left. \frac{d}{dt} H_m(t) \right|_{t=t_j} \quad (10)$$

After the first iteration the new calculated mode $h^{<p+1,q>}(t)$ has the same properties as the prior mode $c_q(t)$ at the observation limit t_j . So there is no discontinuity at the junction. To ensure, that the following siftings have no impact to the boundary the values $y_{M,0}$, $y_{m,0}$ and the derivations $\dot{y}_{M,0}$, $\dot{y}_{m,0}$ are set to zero for all following iterations.

These conditions for the left boundary ensure, that the modes c_p and the trend $r^{<p>}$ are continuous at the observation limit t_j . With this enhanced boundary conditions, the number of iterations may vary with individual blocks, past modes are not affected due to new extrema, less data is to store and no discontinuities occur.

4.3. Blockwise EMD algorithm

Hermite splines and the proposed boundary conditions allow to calculate a mode blockwise with each upcoming extrema, which is continuous and independent of further samples. This section gives a description of the observation window and its movements.

The blockwise EMD needs at least five extremes to calculate a piece of the mode between at least the last two extremes. Figure 3 shows an example of the observation window at the first sifting iteration and the resulting mode $c_q(t)$. The proposed boundary conditions (9,10) are used to describe the left

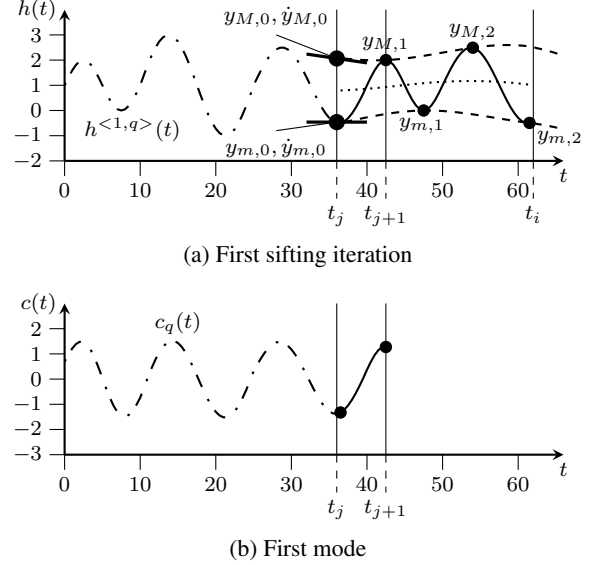


Fig. 3. Enhanced boundary conditions

edge of the window. At the time t_i a new extrema $y_{m,2}$ appears and allows the final description of the lower envelope between $y_{m,0}$ and $y_{m,1}$. The upper envelope is fixed between t_j and t_{j+1} by its maxima $y_{M,0}$ and $y_{M,1}$. The resulting piece of the mode, which is independent of new occurring samples, is located between the two last extremes at t_j and t_{j+1} . After the calculation the observation window shrinks from t_j to t_{j+1} and raises again with each new sample till a next extrema appears.

Figure 3 b shows the blockwise calculated mode with a delay of the last four extrema. However, for an online application - meaning an estimation of the instantaneous frequency with each new sample, an estimation of the mode $c_q(t)$ is necessary. Therefore the extrapolation of the trend $r^{<q>}(t)$ may be appropriate. The extrapolated trend $r^{<q>}(t)$ is subtracted from the signal $y(t)$ to estimate the mode $c_q(t)$. With each new extrema the estimation of the mode and the trend are updated by the blockwise EMD calculation.

5. EXAMPLE

As proposed, Hermite splines for interpolation of extrema and enhanced boundary conditions are used to decompose a synthetic signal. After the online decomposition of the signal the resulting mode is analysed by a frequency estimation method (DESA) based on the Teager Kaiser energy operator introduced in Section 2. The analysed signal is defined as follows:

$$y(t) = \begin{cases} 1.0 \sin(0.628t) + 1 & 0 \leq t < 10 \\ 2.0 \sin(0.418t) + 1 & 10 \leq t < 25 \\ 1.5 \sin(0.418t) + 1 & 25 \leq t < 40 \\ 1.0 \sin(0.628t) + 1 & 40 \leq t < 50 \\ 1.5 \sin(0.628t) + 1 & 50 \leq t < 60 \end{cases} \quad (11)$$

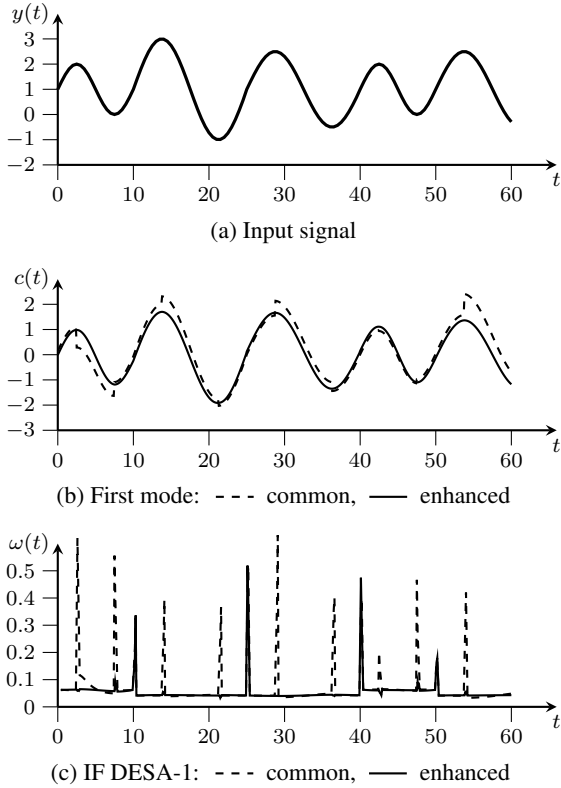


Fig. 4. Application of online EMD and IF estimation

It represents a non-stationary signal with frequency and/or amplitude modulated components as well as a time-varying tone or carrier. The example was mainly chosen simply to put the focus on the discontinuities. This signal was used throughout the article and is illustrated in Fig. 4a. For comparison purposes the input signal is decomposed online using the blockwise EMD scheme with commonly used and improved boundary conditions using Hermite spline interpolation. Fig. 4b shows the resulting first IMF for both online decomposition schemes. As expected, due to enhanced boundary conditions (9, 10), the proposed version based on Hermite splines eliminates the discontinuities at rear block edges (located at extrema). The resulting effects regarding instantaneous frequency estimation are demonstrated in Fig. 4c. Frequency estimation based on the common decomposition approach (dashed) leads to artificially introduced artifacts. The herein proposed approach identifies the inherent frequencies accurately with only high frequency components at points in time where the amplitude or the frequency is switched, see (11).

6. CONCLUSION

The accuracy of instantaneous frequency estimation of non-stationary signals is most often affected by an inherent tone signal. This effect is demonstrated by a fast four-sample energy-

based frequency estimation algorithm. However, a proposed online version of the EMD scheme was addressed to extract zero-mean AM/FM modes. To eliminate disturbing discontinuities in the individual modes enhanced boundary conditions are introduced based on Hermite splines. The benefits are less data for storage, a varying number of sifting-iterations for each block and an improved accuracy regarding instantaneous frequency estimation.

ACKNOWLEDGEMENTS

The authors would like to acknowledge the financial support of the "COMET - Competence Centers for Excellent Technologies Programme" of the Austrian Federal Ministry for Transport, Innovation and Technology (bmvit), the Austrian Federal Ministry of Science, Research and Economy (bmwfw), the Austrian Research Promotion Agency (FFG), the Province of Styria and the Styrian Business Promotion Agency (SFG).

REFERENCES

- [1] N. E. Huang, Z. Shen, S. R. Long, M. L. Wu, H. H. Shih, Q. Zheng, N. C. Yen, C. C. Tung, and H. H. Liu, "The empirical mode decomposition and the hilbert spectrum for nonlinear and non-stationary time series analysis," *Proc. R. Soc. Lond. A*, vol. 454, pp. 903–995, November 1998.
- [2] G. Rilling and P. Flandrin, "On the influence of sampling on the empirical mode decomposition," in *IEEE Proceedings of the international Conference on Acoustics, Speech and Signal Processing, ICASSP*, Toulouse, France, 2006, pp. 444–447.
- [3] A. Y. Ayenu-Prah and N. O. Attoh-Okine, "Comparative study of hilbert-huang transform, fourier transform and wavelet transform in pavement profile analysis," *Vehicle System Dynamics*, vol. 47, no. 4, pp. 437–456, April 2009.
- [4] R. T. Rato, M. D. Ortigueira, and A. G. Batista, "On the hht, its problems, and some solutions," *Mechanical Systems and Signal Processing*, vol. 22, no. 1, pp. 1374–1394, January 2008.
- [5] J.F. Kaiser, "On a simple algorithm to calculate the 'energy' of a signal," *Acoustics, Speech, and Signal Processing*, vol. 1, pp. 381–384, 1990.
- [6] Byeong-Gwan Iem, "Generalization of an instantaneous frequency estimator based on the higher order differential energy operator," *TENCON 2008 - 2008 IEEE Region 10 Conference*, vol. 10, pp. 1–4, 2008.
- [7] R. N. Meeson, "Hht sifting and adaptive filtering," Tech. Rep., Institute For Defense Analyses, 2003.
- [8] Cleve Moler, *Numerical Computing with Matlab*, Society for Industrial and Applied Mathematics, 2004.